16th World Conference on Earthquake Engineering, 16WCEE 2017

Santiago Chile, January 9th to 13th 2017

Paper N° 311

Registration Code: S-P1464504834

DIAGONAL STRUT MECHANISM OF URM WALL BUILT IN RC FRAMES FOR MULTI BAYS

H. Choi(1), Y. Sanada(2), Y. Nakano(3), K. Matsukawa(4)

(1) Research Associate, Institute of Industrial Science, The University of Tokyo, choiho@iis.u-tokyo.ac.jp
(2) Associate Professor, Osaka University, sanada@arch.eng.osaka-u.ac.jp
(3) Professor, Institute of Industrial Science, The University of Tokyo, iisnak@iis.u-tokyo.ac.jp
(4) Research Associate, Institute of Industrial Science, The University of Tokyo, mtkw@iis.u-tokyo.ac.jp

Abstract

The authors have studied the in-plane seismic performance of one-story, one-bay RC frames with URM wall, and investigated the failure mechanism forming a diagonal strut in the walls. They discussed a simple approach to evaluate the lateral resistances of infill walls.

The objectives of this study are to clarify the in-plane and out-of-plane behaviors of infill walls, and to propose a reinforcing system to prevent the infill walls from out-of-plane failure. The current paper reports on in-plane cyclic static tests on one-story, one-bay and one-story, two-bay specimens representative of Turkish RC moment resisting frame models infilled URM walls, and investigates the lateral force resisting mechanisms of the infill walls using an experimental method to identify the diagonal compressive strut formation. Based on the results of the tests, the following major findings were obtained.

(1) The proposed method of evaluating an equivalent diagonal strut based on the strain measurements can accurately estimate the wall strengths for the 1 bay and 2 bay specimens throughout the loading cycle.

(2) Two independent diagonal struts were formed in the 2 bay specimen. This result supports the effectiveness of analytical modelding by single strut replacement for infill in multi-bay farmes.

(3) The FEMA procedure underestimated the lateral strengths of both specimens.

Keywords: diagonal strut; URM wall; multi bays; RC frame; in-plane seismic performance

1. Introduction

In some regions of Asia, Europe, and Latin America where earthquakes frequently occur, serious earthquake damage is commonly found resulting in catastrophic building collapse. Such damaged buildings often have unreinforced masonry (URM) walls, which are considered non-structural elements in the structural design stage, and building engineers have paid less attention to their effects on structural performance although URM walls may interact with boundary frames. The evaluation of seismic capacity of URM walls built inside boundary frames is therefore urgently necessary to mitigate earthquake damage for those buildings.

For this purpose, the authors have previously studied the in-plane seismic performance of one-story, one-bay RC frames with URM wall, and investigated the failure mechanism forming a diagonal strut in the walls. They have discussed a simple approach to evaluate the lateral resistances of infill walls [1, 2].

The objectives of this study are to clarify the in-plane and out-of-plane behaviors of infill walls, and to propose a reinforcing system to prevent the infill walls from out-of-plane failure. This paper reports on in-plane cyclic static tests on one-story, one-bay and one-story, two-bay specimens and the results of such tests, particularly on the diagonal strut of the infill walls and the shear strengths.

2. Experimental Program

2.1 Prototype building and scaled specimens

To improve the seismic performance of URM infill walls, a research project was initiated in collaboration between European and Japanese universities, under JST (Japan Science and Technology Agency) Concert-Japan (Connecting and Coordinating European Research and Technology Development with Japan) project. A building in Turkey was selected as a reference building and 1/4-scale models were prepared. Fig.1 shows the outline of the reference building. The building is a 5-story RC building in Turkey, with the plan dimensions of 23m by 16m and each story height of 3m. As shown in the figure, the interior middle frame in the longitudinal direction in the first story was focused to design the prototype speimen. In this study, however, two types of specimens were designed, as shown in Fig.2: one-story, one-bay specimen (1 bay specimen) and one-story, two-bay specimen (2 bay specimen).

Fig.3 shows the details of the 1 bay speimen. The area ratios of longitudinal reinforcement and shear reinforcement to the cross-sectional area were designed to be approximately equal to those of the reference building. The upper beam with a T-shape section, considering an effective slab width, was designed to fail in flexure, where the shear-to-flexural strength ratio (Q_{SU} / Q_{MU} [3]) and the flexural stiffness were equivalent to those of the reference building. The masonry unit was also scaled by 1/4 as shown in Fig.3. In this study, the concrete block (CB) unit was employed instead of the hollow clay brick generally used in Turkey. However, the cement-to-sand ratio was adjusted so that the strength and stiffness of three layered CB prism specimens corresponded to those of the full-scale whose detail was described in the reference [4].

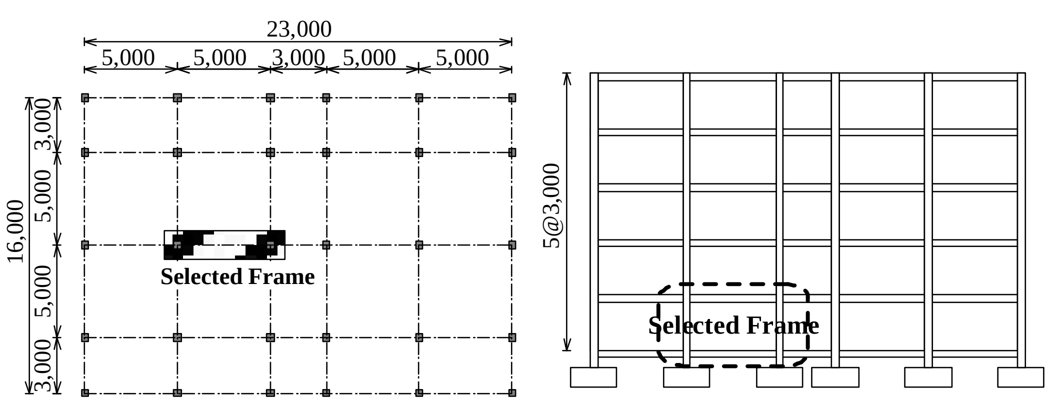

Fig. 1 – Outlines of the reference building (unit: mm)

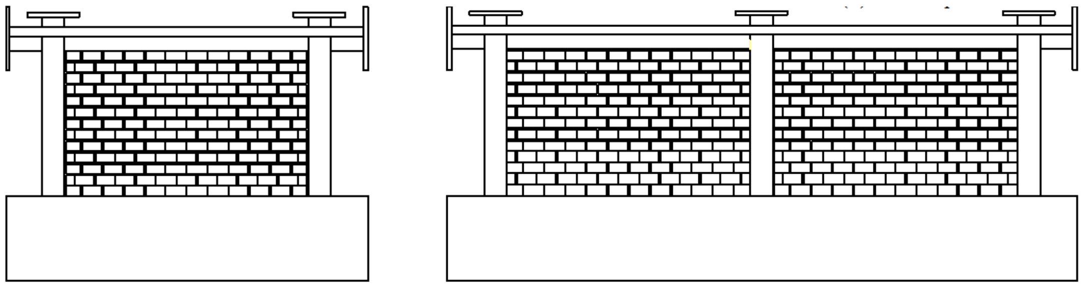

(a) 1 bay specimen (b) 2 bay specimen

Fig. 2 – Elevations of the specimens

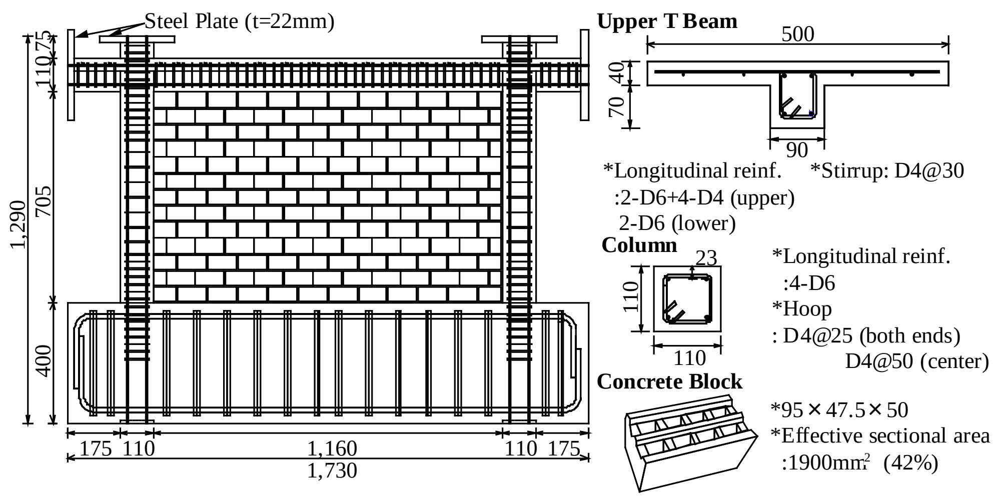

Fig. 3 – Details of the 1 bay specimen

2.2 Material characteristics

Table 1 through Table 3 show the material test results, where the values present the mean value of 3 samples from each test. Although the design compressive strength of concrete was 18 N/mm^2, the value of test cylinders exceeded it, as shown in Table 1. The yield stresses of reinforcements showed values that were 35% higher than the nominal yield stress, as shown in Table 2. The compressive strength and Young's modulus from the three layered CB prism tests were 8.4 N/mm^2 and 9.6×10^3 N/mm^2, respectively, as shown in Table 3. The results obtained from the material tests were used in estimating the section capacities.

Table 1 – Material test results of concrete

Compressive strength, f'_c [N/mm^2]	Young's modulus, E_c [N/mm^2]
24.1	2.1×10^4

Table 2 – Material test results of steel bars

	Yield strength, f_y [N/mm^2]	Young's modulus, E_s [N/mm^2]
D4	401	2.1×10^5
D6	407	2.0×10^5

Table 3 – Material test results of masonry prisms (The values for the gross cross-sectional area of CB unit)

Compressive strength, f_m [N/mm^2]	Young's modulus, E_m[N/mm^2]
8.4	9.6×10^3

2.3 Test setup and loading protocol

A loading system for the in-plane cyclic static tests is shown in Fig.4. Lateral loads in the positive and negative directions were applied from the left and right ends of the beam with hydraulic actuators. Two vertical actuators were installed to apply a constant axial load of 35 kN (2.9 N/mm^2) on the top of each column, and a distributed load of 5.9 kN/m (in total 7.5 kN) was also applied considering a design dead load. Two pantagraphs were used to provide out-of-plane stability during the tests. Fig.5 shows a lateral loading protocol, which was controlled by a drift angle R, which was defined as a lateral drift Δ at the center of the uppermost beam divided by the height from the bottom of the specimen, H, as shown in Fig.4.

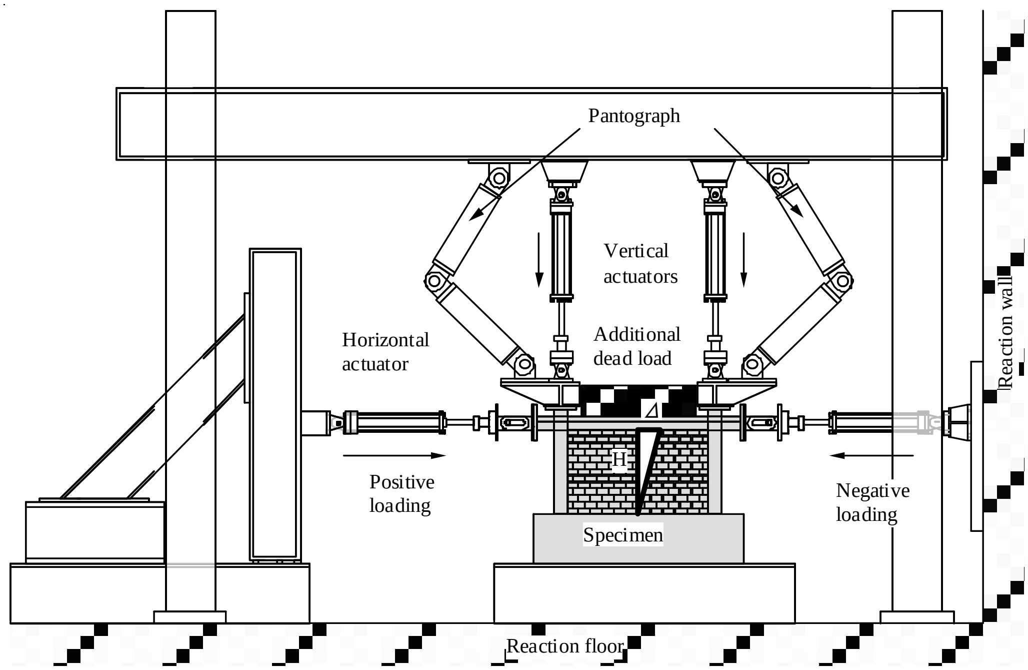

Fig. 4 – Loading system for the 1 bay specimen

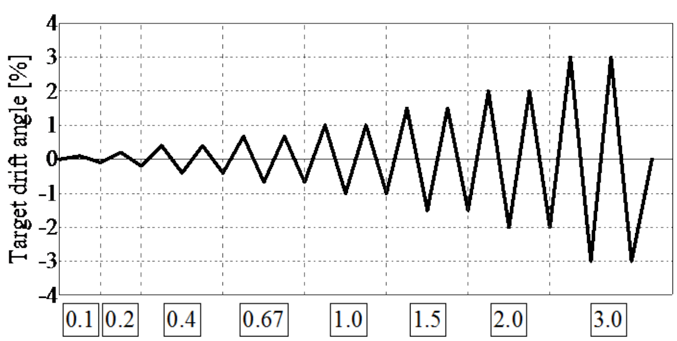

Fig. 5 – Lateral loading protocol

2.4 Instrumentation plan

A key objective of the tests was to capture three-axis strain gauge data for all the blocks in the 1 bay specimen. Due to limitations in the measurement equipment, it was not possible to measure three-axis strain data for all the blocks of the 2 bay specimen; therefore, approximately a half of the blocks were selected to evaluate the strut mechanism in the positive loading direction according to the method proposed in the previous study [1]. Fig.6 shows strain gauge arrangements for both specimens.

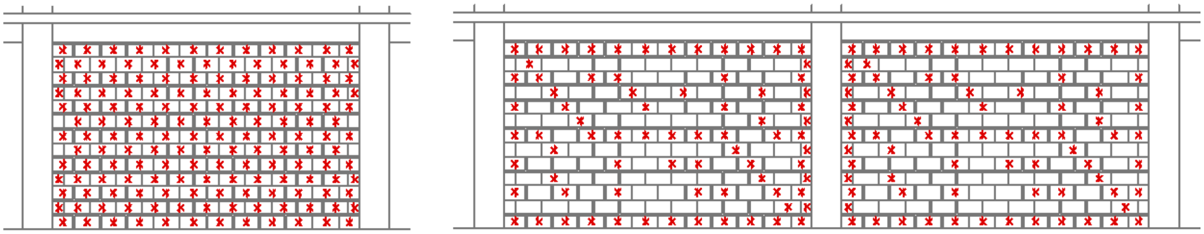

(a) 1 bay specimen (b) 2 bay specimen

Fig. 6 – Elevations of the specimens

3. Failure Patterns and Lateral Load-Drift Relationships

Figs. 7 and 8 show the final crack patterns and the lateral load-drift relationships of both specimens, respectively.

3.1 1 bay specimen

Focusing on the infill wall, horizontal cracks and step-wise cracks occurred on the wall from a small drift angle of 0.1%, most of which were observed on the joint mortar. These cracks developed until the maximum strengths were recorded, and widely opened beyond drifts at the peak strengths. Crushing and spalling off of the blocks caused significant strength drops of the specimens. In the boundary frame, flexural cracks were observed to not only both column ends but also the middle height of the columns, which indicated that the wall formed a compression strut along the diagonal direction. The maximum strengths reached 52.2kN and -58.7kN at 1% and -1.5%, respectively. The deformation capacities, which were defined as the drift when the lateral resistance decreased to 80% of the maximum strength, were 2% and -3% in the positive and negative directions, respectively.

In order to calculate the lateral strength of both columns, which is shown in Fig.8(a), the initial stiffness (K_c), secant stiffness ($\alpha_y \cdot K_c$), and cracking moment (M_c) of a column were calculated according to the method described in reference [5]. The ultimate bending moment M_u of columns was also calculated based on the plane-section assumption setting the ultimate strain ε_{cu} at the compression fiber of concrete equal to 0.003 with an equivalent rectangular stress block coefficient 0.85 [5]. Based on the curvature distributions of columns calculated from the test data, the effective height of tensile column was assumed as $0.5h_0$ (h_0: column height (=705 mm, as shown in Fig.3)), while that of the compression column was assumed as h_0. The shear strength V_C of CB wall is then calculated according to Eqs. (1) and (2) [6], and the sum of shear force of RC columns and CB wall is shown in Fig.8(a), which does not show good agreement with the overall lateral strength.

$$V_C = a_{eq} \cdot t \cdot f_m \cdot \cos\theta_m \tag{1}$$

$$a_{eq} = 0.175 \cdot \left(\frac{4 \cdot E_c \cdot I_c \cdot h_m}{E_m \cdot t \cdot \sin 2\theta_m \cdot h^4} \right)^{0.1} \cdot l_d \tag{2}$$

wherein Eqs. (1) and (2), a_{eq}: the equivalent strut width, t: the thickness of CB wall, f_m: 50% of prism strength, θ_m: the angle of CB wall height to length, E_c: the Young's modulus of concrete, I_c: the moment of inertia of column, h_m: the height of CB wall, E_m: the Young's modulus of CB prism, h: the column height, and l_d: the diagonal length of CB wall, respectively.

3.2 2 bay specimen

This specimen had higher initial stiffness and maximum strength than the 1 bay specimen. Compared with the 1 bay specimen, the maximum strength was approximately twice, which was 104.4 kN at the drift angle of 0.4%. Many cracks were observed on the ends of the middle column, which resulted from compression forces applied on the column by both sides of infill walls. Cracks patterns in both walls were similar to that of the 1 bay specimen.

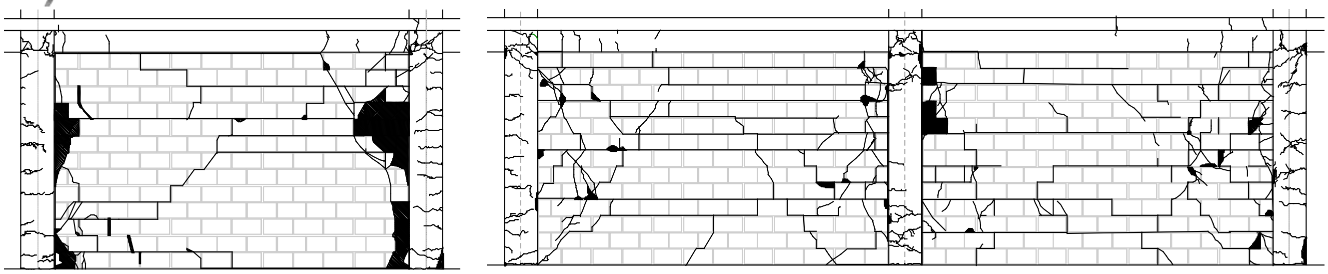

(a) 1 bay specimen (b) 2 bay specimen

Fig. 7 – Final crack patterns

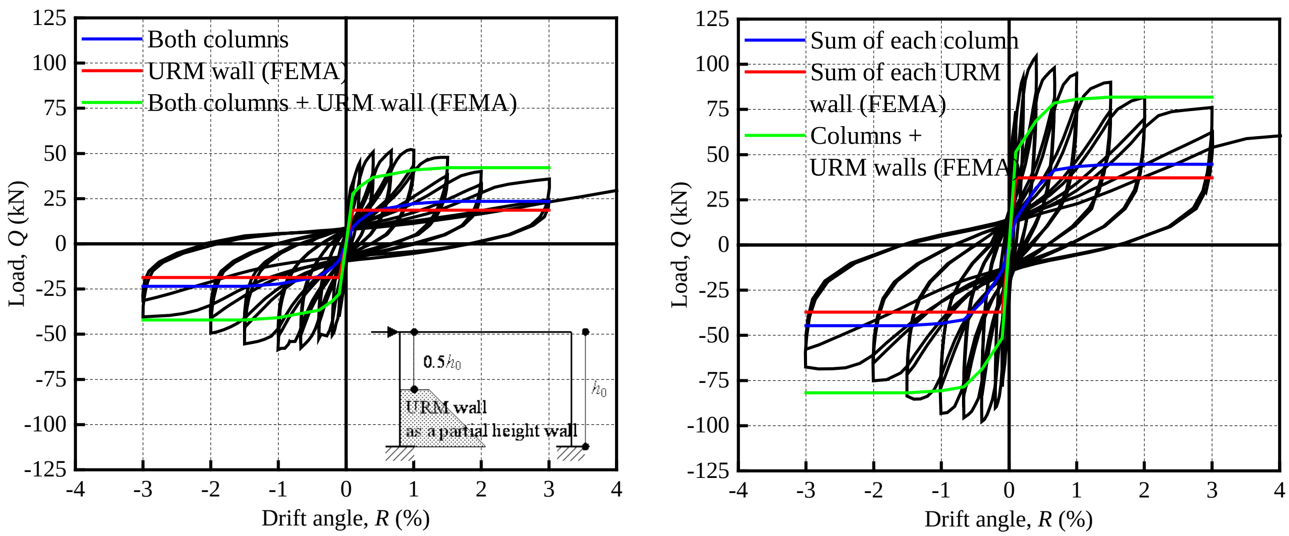

(a) 1 bay specimen (b) 2 bay specimen

Fig. 8 – Lateral strength and drift angle relations

4. Equivalent Diagonal Strut and Shear Strength of URM Infill

Calculations for the strut parameters were made as per the following procedure. For detailed discussions about the method, kindly see Reference [1].

4.1 Principal compressive strain ε_j and its angle θ_j of each CB unit

The principal compressive strain ε_j and its angle θ_j for each CB unit are first calculated from the strain values measured by the 3-axis strain gauges on CB wall. Fig.9 shows the principal compressive strain and its angle for each CB unit at the drift angle of 0.4% in both specimens. As can be found from the figure, most principal compressive strain of CB units were oriented diagonally with respect to the horizontal line.

4.2 Main diagonal strut angle θ of CB wall

The main diagonal strut angle was estimated from the principal compressive strain and its angle for each CB unit. In this study, the average of the principal compressive angle weighted with its strain was employed to calculate the main diagonal strut angle θ, as shown in Eq. (3).

$$\theta = \left(\sum_{j=1}^{l} \varepsilon_j \times \theta_j \right) / \sum_{j=1}^{l} \varepsilon_j \tag{3}$$

where, ε_j and θ_j: the principal compressive strain and angle for a CB unit, l: the number of CB units with θ_j between 0 and 90 degrees, respectively.

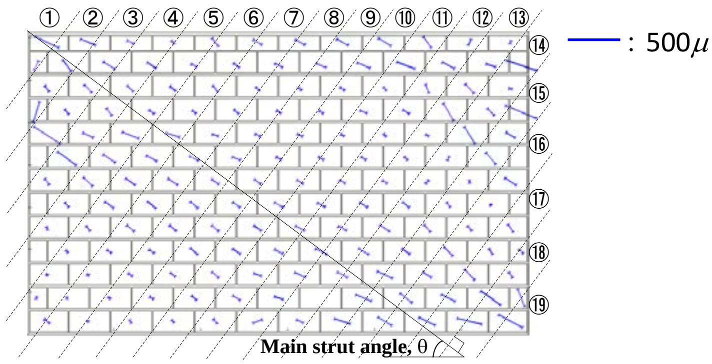

(a) 1 bay specimen

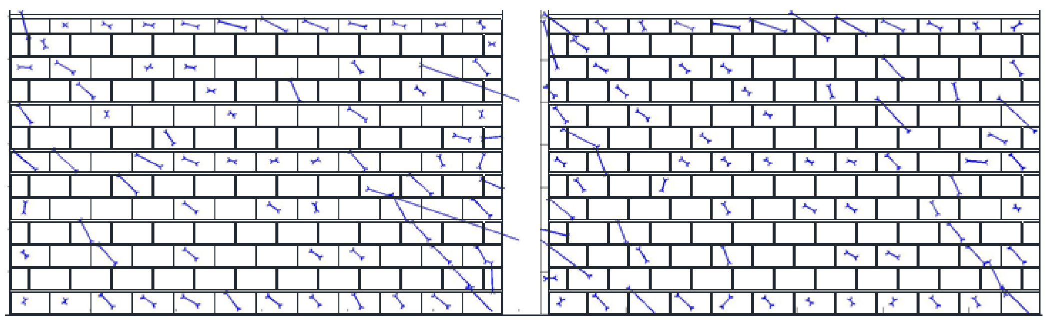

(b) 2 bay specimen

Fig. 9 – Principal compressive strain distributions (0.4%, positive direction loading)

4.3 Principal compressive strain distribution along the diagonal strut

The CB wall was divided into 19 sections at equal intervals in the diagonal direction, as shown in Fig.9(a), and the mean value of principal compressive strains ε_i of CB units included in section i was calculated, as shown in Fig.10. As can be seen in Fig.10, the mean value ε_i shows a nearly symmetric distribution with concave shape at the drift angle of 0.4% in both specimens. The average value of principal compressive strain ε_i of 19 sections was defined as the average principal compressive strain ε_m, and this value was assumed to be the representative strain of the CB wall.

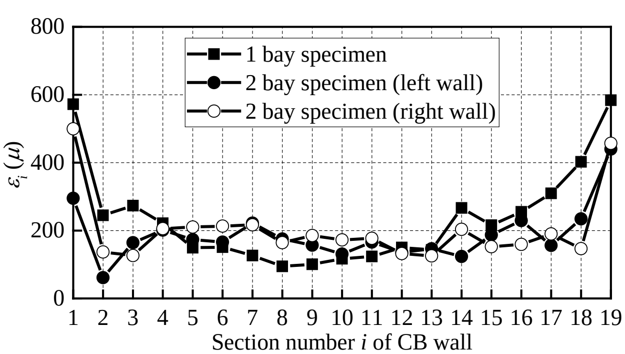

Fig. 10 – Mean value of comp. strain in each section

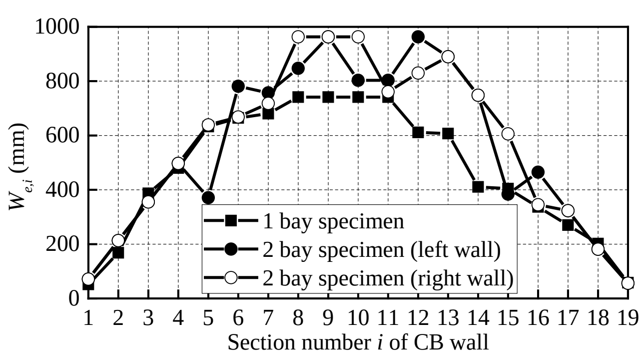

Fig. 11 – Effective strut width in each section

4.4 Effective strut width and equivalent diagonal strut width

The effective strut width $W_{e,i}$ in each section at 0.4% drift loading is shown in Fig.11. It was defined as the outmost distance of CB units having principal angle in the range of 0 through 90 degrees. In both specimens, the effective strut width shows a nearly symmetric distribution with convex shape as shown in the figure. The equivalent diagonal strut width W_{eq} is then evaluated according to Eq. (4), which assumes that the same compression force P is applied to the equivalent strut section, as shown in Fig. 12.

$$W_{eq} = \left(\sum_{i=1}^{n} (\varepsilon_i \times W_{e,i}) \right) / \sum_{i=1}^{n} \varepsilon_i \, (n = 19) \tag{4}$$

where, ε_i and $W_{e,i}$: the mean value of principal compressive strain and effective strut width in section, respectively.

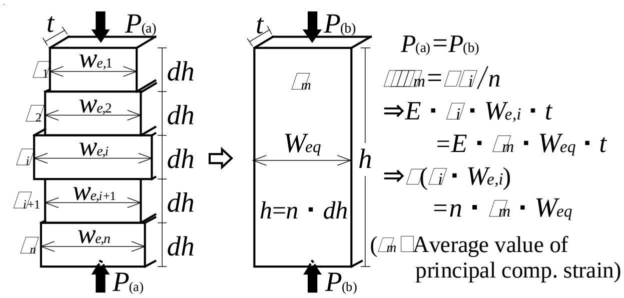

(a)Original strut (b)Equivalent strut

Fig. 12 – Equivalent diagonal strut width

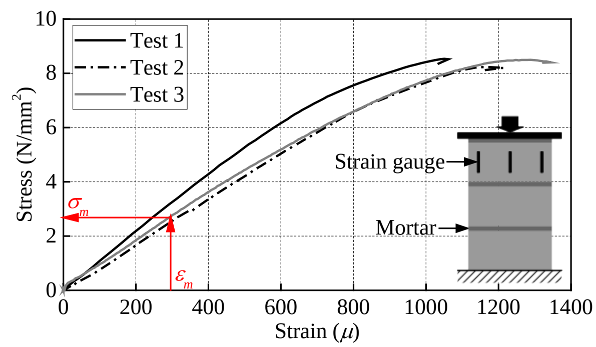

Fig. 13 – σ_m - ε_m relationship

4.5 Central axis of diagonal strut C_y

The central axis distance C_y was calculated using the centroid distance C_{yi} at each section. C_{yi} and C_y were calculated using Eqs. (5) and (6), respectively.

$$Cy_i = \left(\sum_{i=1}^{l} \varepsilon_j \times y_j \right) / \sum_{i=1}^{l} \varepsilon_j \tag{5}$$

$$Cy = \left(\sum_{i=1}^{n} \varepsilon_i \times Cy_i \right) / \sum_{i=1}^{n} \varepsilon_i \, (n = 19) \tag{6}$$

where, y_i: the distance to the center of principal compressive strain in section i perpendicular to the main strut angle.

4.6 Estimation of shear strength of CB wall

The lateral strength of an URM infill wall, based on an equivalent diagonal strut, was calculated by Eq. (7). In that equation, σ_m is the principal compressive stress corresponding to the average principal compressive strain ε_m of the equivalent diagonal strut. In this study, the stress (σ_m)-strain (ε_m) relationship was obtained from the 3-layerd prism tests, as shown in Fig.13.

$$V_c = W_{eq} \cdot t \cdot \sigma_m \cdot \cos\theta \tag{7}$$

where, W_{eq}: the equivalent strut width, θ: the main strut angle, σ_m: the stress corresponding to the equivalent strut's principal compressive strain ε_m, based on three layered prism tests, t: the thickness of the wall (48 mm), respectively.

5. Shear Strength of Overall Frame

The overall lateral load and deflection relationship in both specimens were finally demonstrated based on the estimated behavior of RC columns (Fig.8) and the lateral load V_c carried by the CB wall from Eq. (7) and Fig.13.

Figure 14 shows the equivalent diagonal strut at the drift angle of 0.4% for both specimens claculated by the proposed method stated in Section 4. As shown in the figure, the calcurated values of the main diagonal strut angle θ, central axis distance C_y and equivalent diagonal strut width W_{eq} for each wall in the two specimens were similar to one another. In particular, in the case of the 2 bay specimen, the compressive struts were individually formed in each wall. This result menas that multi-bay walls can be modeled based on an equivalent single strut in each bay.

Figure 15 shows the oveall lateral strength – deflection relationships for both specimens calculated by the proposed method together with the test results. As can be seen in the figure, the overall lateral strengths calculated by the proposed method show good agreement with the test results throughout the loading cycle.

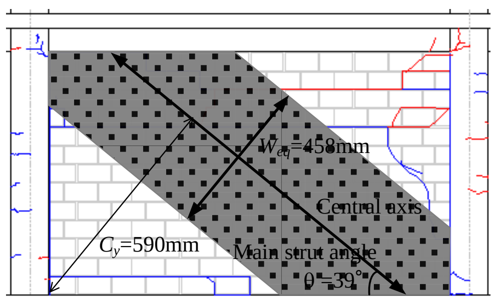

(a) 1 bay specimen

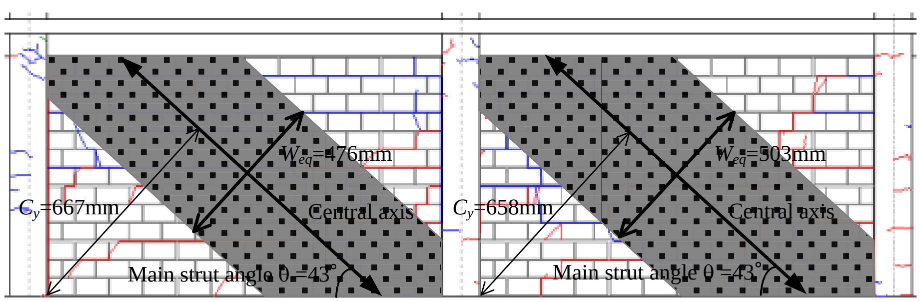

(b) 2 bay specimen

Fig. 14 – Equivalent diagonal strut in both specimens (0.4%)

6. Conclusions

The current paper reports on the experimental test models representing the URM infill walls in Turkish RC moment resisting frames, and investigates the lateral force resisting mechanisms of the infill walls using an experimental method to identify the diagonal compressive strut formation. The following major findings were obtained.

(1) The proposed method for evaluating an equivalent diagonal strut based on the strain measurements can accurately estimate the wall strengths for the 1 bay and 2 bay specimens throughout the loading cycle.

(2) Two independent diagonal struts were formed in the 2 bay specimen. This result supports the effectiveness of analytical modelding by single strut replacement for infill in multi-bay farmes.

(3) The FEMA procedure underestimated the lateral strengths of both specimens.

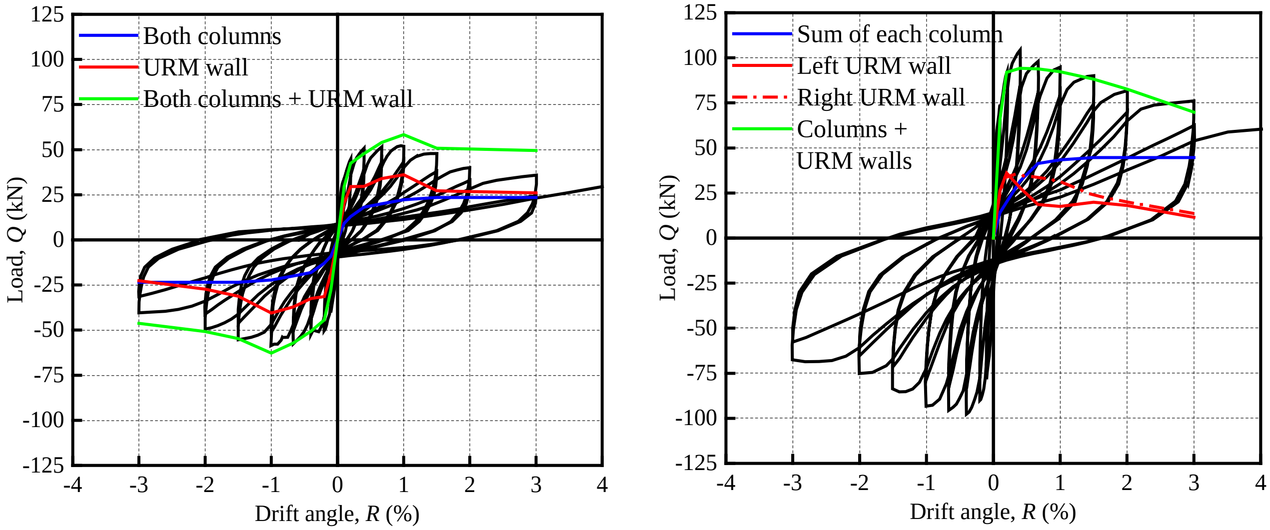

(a) 1 bay specimen (b) 2 bay specimen

Fig. 15 – Lateral strength evalution of both specimens

7. Acknowledgements

The project was funded by CONCERT-Japan (Connecting and Coordinating European Research and Technology Development with Japan) project (Project leader: Professor Polat Gulkan of Cankaya Unversity, Turkey, Project leader in Japan: Professor Yoshiaki Nakano) under JST (Japan Science and Technology Agency). The authors are greatly thankful for the finalcial support.

8. References

[1] Jin K, Choi H, Takahashi N, Nakano Y (2012): Failure Mechanism and Seismic Capacity of RC Frames with URM Wall considering Its Diagonal Strut. *Proc. 15th World Conference of Earthquake Engineering (WCEE), International Association of Earthquake Engineering*, Lisbon, Portugal.

[2] Jin K, Choi H, Nakano Y (2016): Experimental Study on lateral Strength Evaluation of Unreinforced Masonry-Infilled RC Frame. *Earthquake Spectra*, DOI: http://dx.doi.org/10.1193/100714EQS152M.

[3] Kabeyasawa T, Shiohara H, Otani S, Aoyama H (1983): Analysis of the Full-scale Seven-story Reinforced Concrete Test Structure. *Journal (B)*, the Faculty of Engineering, University of Tokyo, Vol. XXXVII, No.2, pp.432-478.

[4] Gülkan P, Binici H, Sucuoğlu A, Taghipour O, Demirel S, Tanışer O, Güneş M, Ismail E, Fehling Y, Nakano Y, Sanada Y, Choi H (2015): An Innovative Tie System for Improving the Monolithic Behavior of Masonry In-filled Reinforced Concrete Frames (INFILTIE)". *3rd Turkish National Conference on Earthquake Engineering and Seismology*, Izmir, Turkey.

[5] Architectural Instite of Japan (AIJ) (2010). *AIJ Standard for Structural Calcuation of Reinforced Concerete Structures.*

[6] FEMA 306 (1998). *Evaluation of earthquake damaged concrete and masonry wall buildings*. Applied Technology Council (ATC-43 Project).